Magnetic Energy Levels in an Energy Band with Inversion Asymmetry Splitting

LAURA M. ROTH
General Electric Research and Development Center, Schenectady, New York
(Received 23 April 1968)

We consider an energy band which is spherical except for a term giving the inversion asymmetry splitting possible in the zinc-blende structure. This splitting is small but very anisotropic, so that the classical cyclotron orbits on the split Fermi surfaces are complicated and sometimes cross. We solve for the magnetic levels of the system when the magnetic field is along the three principle directions. The results for ⟨111⟩ and ⟨100⟩ differed considerably from the classical picture. The calculation supports the proposal of Groves and Wyatt that the beating observed in the Shubnikov–de Haas effect in HgSe by Whitsett is due to inversion asymmetry splitting. The beat pattern was fairly well accounted for. A splitting parameter γ of 0.085 was found for Whitsett's 1.3×10^{18}-cm^{-3} sample, where $\frac{1}{2}\gamma k_F$ is the maximum radial splitting of the Fermi surface.

INTRODUCTION

IN a recent paper,[1] it was proposed that the beating observed by Whitsett[2] in the Shubnikov–de Haas (SdH) effect in n-type HgSe can be explained by inversion asymmetry splitting. As has been discussed previously[1,3,4] this splitting is due to a combination of spin orbit interaction and the antisymmetric potential associated with the dissimilar basis atoms of the zinc-blende lattice. In this article we shall add to the evidence in support of the proposal by calculating exactly the magnetic levels for a band with inversion asymmetry splitting.

We first summarize the experimental results of Whitsett, some of which are reproduced in Fig. 1. When **B** was rotated in a ⟨110⟩ plane, beating occurred for directions of **B** other than ⟨110⟩ in samples of sufficiently high electron concentration. When **B** was along ⟨100⟩, a single node was observed in the range of field strength studied; while for B along ⟨111⟩, one or two nodes were observed. The anisotropy of the period was found to be quite small, which Groves and Wyatt[5] showed to rule out another possible explanation of the beating, namely a severe warping of the Fermi surface. The one complete beat observed in the ⟨111⟩ direction (see Fig. 1) had a node spacing of 28 oscillations. On the basis of a classical model the two Fermi surface cross sections thus apparently differed by $3\frac{1}{2}\%$. This indicates the order of magnitude of the effect; we shall revise the exact result with the present calculation. One further point is the fact that the beats are not evident in the lowest concentration samples. This may be related to the k dependence of the splitting, but is also partly due to the fact that fewer oscillations are seen in the low concentration samples. The matter will be discussed further below.

EFFECTIVE HAMILTONIAN

In I we introduced a simplified 2×2 Hamiltonian to treat the problem:

$$\mathcal{H}=\frac{\hbar^2k^2}{2m^*}+\frac{\hbar\omega_s\boldsymbol{\sigma}\cdot\mathbf{B}}{2B}+\frac{\gamma\hbar^2}{2m^*k_F}[(\sigma_xk_y-\sigma_yk_x)k_xk_y+(\sigma_yk_z-\sigma_zk_y)k_yk_z+(\sigma_zk_x-\sigma_xk_z)k_xk_z]. \quad (1)$$

Here $\boldsymbol{\sigma}$ is a Pauli spin vector, and $\mathbf{k}$ is the kinetic momentum operator $\mathbf{p}+e\mathbf{A}/c$, with $\mathbf{A}$ the vector potential of the magnetic field $\mathbf{B}$. The first term in Eq. (1) is the unperturbed band energy, assumed spherical. The second term is the spin energy, assumed isotropic, with ω_s the spin splitting. The third term gives the inversion asymmetry splitting. In the absence of a magnetic field,

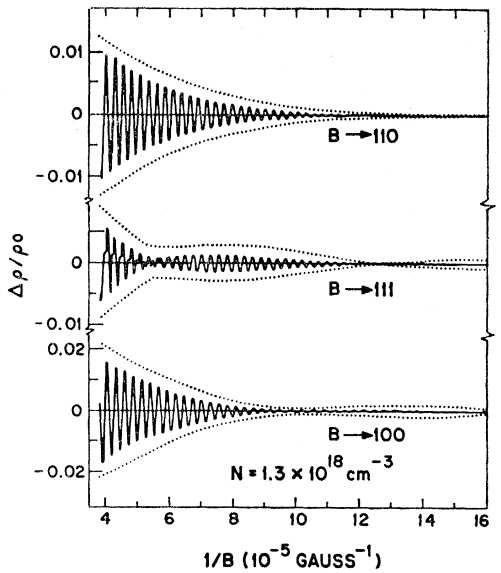

FIG. 1. Oscillatory component of magnetoresistance of Whitsett's HgSe sample L with electron concentration $N=1.34\times10^{18}$ cm^{-3}. Solid curves are for 4.2°K; dotted curves are envelopes of oscillations at 1.2°K. See C. R. Whitsett, Phys. Rev. 138, A829 (1965).

[1] L. M. Roth, S. H. Groves, and P. W. Wyatt, Phys. Rev. Letters 19, 576 (1967), hereafter referred to as I; S. H. Groves, L. M. Roth, and P. W. Wyatt, in *II-VI Semiconducting Compounds, 1967 International Conference*, edited by D. G. Thomas (W. A. Benjamin, Inc., New York, 1967), p. 1069.
[2] C. R. Whitsett, Phys. Rev. 138, A829 (1965).
[3] G. Dresselhaus, Phys. Rev. 100, 580 (1955); R. H. Parmenter, *ibid.* 100, 573 (1955).
[4] E. O. Kane, J. Phys. Chem. Solids 1, 249 (1957); in *Semiconductors and Semimetals*, edited by R. K. Willardson and A. C. Beer (Academic Press Inc., New York, 1966), Vol. 1.
[5] S. Groves and P. Wyatt, unpublished calculation discussed in I and in the Acknowledgment of this paper.

the eigenvalues of Eq. (1) are

$$\epsilon_{\pm}=\frac{\hbar^2k^2}{2m^*}\left\{1\pm\frac{\gamma}{k^2k_F}\times[k^2(k_x^2k_y^2+k_x^2k_z^2+k_y^2k_z^2)-9k_x^2k_y^2k_z^2]^{1/2}\right\}, \quad (2)$$

so that $\gamma\epsilon_F$ is the maximum $(k\|\langle 110\rangle)$ energy splitting near the Fermi level ϵ_F. Or, to first order, $\frac{1}{2}\gamma k_F$ is the maximum radial splitting in k at the Fermi momentum k_F.

We are neglecting warping, which is small compared to the dimensions of the Fermi surface. The other approximations we shall make are related to the assumption that $\gamma\ll 1$. Thus, although the components of k do not commute $([k_x,k_y]=ieB/\hbar c)$, we can neglect this fact in the γ term as it contributes terms of order $\gamma\hbar\omega_c$, where ω_c is the cyclotron frequency for $\gamma=0$, and is therefore always small compared to the level spacing. We shall also equate the magnitude of $\mathbf{k}$ to the Fermi momentum k_F wherever necessary in this term. In particular, γ depends on k in general[1,3,4] and we evaluate it at k_F. The same applies to the spin term.

In Eq. (1) we are neglecting nonparabolicty, but this is possible to modify by suitably interpreting γ. For the nonparabolic case, let us define γ by writing

$$\mathcal{H}=\epsilon(k^2)+\gamma(\partial\epsilon/\partial k^2)g(\boldsymbol{\sigma},\mathbf{k})/k+\hbar\omega_s\boldsymbol{\sigma}\cdot\mathbf{B}/2B, \quad (3)$$

where $g(\boldsymbol{\sigma},\mathbf{k})$ is the contents of the square bracket in Eq. (1). To first order in γ, this can be written

$$\mathcal{H}=\epsilon\left(k^2+\gamma g(\boldsymbol{\sigma},\mathbf{k})/k+\frac{\hbar\omega_s}{\partial\epsilon/\partial k^2}\frac{\boldsymbol{\sigma}\cdot\mathbf{B}}{2B}\right), \quad (4)$$

and we look for the eigenvalues of the argument of Eq. (4), which is essentially identical with Eq. (1). The interpretation of γ as twice the maximum relative splitting in k still holds. We also use the usual result $(eB/\hbar^2ck)(\partial\epsilon/\partial k)$ for the cyclotron frequency.

In I we next transformed coordinates in the Hamiltonian Eq. (1) so that $\mathbf{B}$ is in the k_3 direction, and set $k_3=0$. The resulting Hamiltonians are

$\mathbf{B}\|\langle 100\rangle$:

$$\mathcal{H}=\frac{\hbar^2k^2}{2m^*}+\frac{\hbar\omega_s\sigma_3}{2}+\frac{\hbar^2\gamma}{2m^*k_F}(\sigma_1k_2-\sigma_2k_1)\frac{k_1^2-k_2^2}{2}, \quad (5)$$

$\mathbf{B}\|\langle 110\rangle$:

$$\mathcal{H}=\frac{\hbar^2k^2}{2m^*}+\frac{\hbar\omega_s\sigma_3}{2}+\frac{\hbar^2\gamma}{2m^*k_F}\sigma_3k_2\frac{(2k_1^2-k_2^2)}{2}, \quad (6)$$

$\mathbf{B}\|\langle 111\rangle$:

$$\mathcal{H}=\frac{\hbar^2k^2}{2m^*}+\frac{\hbar\omega_s\sigma_3}{2}+\frac{\hbar^2\gamma}{2m^*k_F}\left\{\left(\frac{2}{3}\right)^{-1/2}\sigma_3k_2\frac{3k_1^2-k_2^2}{2}-\left(\frac{1}{3}\right)^{1/2}\frac{(k_1^2+k_2^2)}{2}(\sigma_1k_2-\sigma_2k_1)\right\}. \quad (7)$$

The classical orbits were depicted in I, and the first question which arose was that of why nodes were observed for the $\langle 100\rangle$ case and not the $\langle 110\rangle$ case, when both sets of classical orbits intersect. From Eq. (6) for $\mathbf{B}\|\langle 110\rangle$, we see immediately that the third term is proportional to σ_3, so that the Hamiltonian is diagonal. The diagonal elements correspond to orbits of equal area which are uncoupled, even though they cross, so that there is no beating. For the $\langle 100\rangle$ case, however, there are off-diagonal elements, and the analysis of these is one purpose of this paper. For $B\|\langle 111\rangle$ the classical theory is meaningful for small enough magnetic fields; however, we have made an exact calculation here also, and we find that magnetic-breakdown effects[6] occur and are important. We first discuss the $\langle 100\rangle$ case.

$\langle 100\rangle$ CASE

For $B\|\langle 100\rangle$ the Hamiltonian has off-diagonal terms, so that we first diagonalize the last term. This can be accomplished by the unitary transformation

$$U=\frac{1}{\sqrt{2}}\begin{pmatrix} ie^{-i\varphi} & -ie^{i\varphi} \\ 1 & 1\end{pmatrix}. \quad (8)$$

This is slightly different from and preferable to the transformation used in I, which involved the double-valued function $e^{i\varphi/2}$. As was pointed out in I, we treat $e^{i\varphi}$ as simply a function of k in transforming the last term in Eq. (5), but must use the operator property in transforming the first term. We introduce creation and destruction operators for harmonic oscillator wave functions,

$$\begin{Bmatrix} a^\dagger \\ a\end{Bmatrix}=\left(\frac{\hbar c}{2eB}\right)^{1/2}(k_1\pm ik_2),$$

with $n=a^\dagger a$, and define $e^{i\varphi}$ and $e^{-i\varphi}$ as the operators $n^{-1/2}a^\dagger$ and $an^{-1/2}$. The latter operators are inverses if we exclude the $n=0$ state, so that U is unitary with this restriction. The transformed Hamiltonian is then

$$\mathcal{H}'=\begin{pmatrix} \frac{\hbar^2k^2}{2m^*}-\frac{\hbar\omega_c}{2}+\frac{\gamma\hbar^2}{2m^*}\frac{(k_1^2-k_2^2)}{2} & \frac{\hbar(\omega_c-\omega_s)}{2} \\ \frac{\hbar(\omega_c-\omega_s)}{2} & \frac{\hbar^2k^2}{2m}-\frac{\hbar\omega_c}{2}-\frac{\gamma\hbar^2}{2m^*}\frac{(k_1^2-k_2^2)}{2}\end{pmatrix}=\hbar\omega_c\begin{pmatrix} n+\frac{1}{4}\gamma(a^2+a^{+2}) & \mu \\ \mu & n-\frac{1}{4}\gamma(a^2+a^{+2})\end{pmatrix}, \quad (9)$$

[6] M. Cohen and L. Falikov, Phys. Rev. Letters **5**, 544 (1960).

where $\mu=1/2(1-\omega_s/\omega_c)$, with $\omega_c=eB/mc$ the cyclotron frequency, and where we have used $k=k_F$.

As was pointed out in I, the off-diagonal terms in Eq. (9) produce a field-dependent coupling between the two elliptical orbits, so that we can expect a reversed magnetic breakdown effect. However, we shall be interested here in actually solving for the eigenvalues of Eq. (9). To this end we find it convenient to make a scale transformation so that one of the elliptical orbits turns into a circular orbit. This can be done exactly, but we need the result essentially only to first order in γ. To this order we let $a\rightarrow a+\frac{1}{4}\gamma a^+$, $a^+\rightarrow a^++\frac{1}{4}\gamma a$. The new operators have the same commutation relations as before to first order in γ. The transformed Hamiltonian is then

$$\mathcal{H}''=\hbar\omega_c\begin{pmatrix} n(1+\gamma^2)^{1/2}+\frac{1}{2}\gamma(a^2+a^{+2}) & \mu \\ \mu & n \end{pmatrix}. \quad (10)$$

Here we have put in the factor $(1+\gamma^2)^{1/2}$ to force the eigenvalues of the two diagonal terms to be exactly equal in order to avoid any spurious beats for larger values of n.

We see that the γ term couples states with the quantum numbers n and $n\pm2$. If we take matrix elements of Eq. (10) between harmonic oscillator functions, we are led to consider an infinite matrix with 2×2 blocks given in the vicinity of n by

$$\mathcal{H}''-\lambda\hbar\omega_c=\hbar\omega_c\left[\begin{array}{cc|cc|cc} (n-4)(1+\gamma^2)^{1/2}-\lambda & \mu & \frac{1}{2}\gamma[(n-2)(n-3)]^{1/0} & 0 & 0 & 0 \\ \mu & n-4-\lambda & 0 & 0 & 0 & 0 \\ \hline \frac{1}{2}\gamma[(n-2)(n-3)]^{1/2} & 0 & (n-2)(1+\gamma^2)^{1/2}-\lambda & \mu & \frac{1}{2}\gamma[n(n-2)]^{1/2} & 0 \\ 0 & 0 & \mu & n-2-\lambda & 0 & 0 \\ \hline 0 & 0 & \frac{1}{2}\gamma[n(n-0)]^{1/2} & 0 & \frac{1}{2}n(1+\gamma^2)^{1/2} & \mu \\ 0 & 0 & 0 & 0 & \mu & n-2 \end{array}\right]. \quad (11)$$

The nondiagonal matrix elements are seen to be close to the diagonal, and because of this it is possible to find a recursion relation for D_n, the determinant truncated after the 2×2 block corresponding to n. If we truncate Eq. (11) and then expand in terms of 2×2 minors from the last two columns, and their complements, using Laplace's development, the following relation results:

$$D_n=\{(n-\lambda)(n(1+\gamma^2)^{1/2}-\lambda)-\mu^2\}D_{n-2} -\{\tfrac{1}{4}\gamma^2n(n-1)(n-2-\lambda)(n-\lambda)\}D_{m-4}. \quad (12)$$

In order to calculate the eigenvalue λ, we must find the roots of D_{n_1} for n_1 sufficiently greater than λ. Actually, it shortens the computation to truncate the determinant below as well as above the eigenvalue. This is readily accomplished by setting $D_{n_0-4}=D_{n_0-4}=1$ to truncate at n_0. The calculation was carried out on the General Electric time-sharing computer, and for each range of eigenvalues n_0 and n_1 were varied until convergence was obtained. We shall discuss the results after considering the $\langle111\rangle$ case.

$\langle111\rangle$ CASE

Essentially, the same method can be applied to the $\langle111\rangle$ case. We first simplify the $(\sigma_1k_2-\sigma_2k_1)$ term in the Hamiltonian by making a unitary transformation with

$$U=\begin{pmatrix} ie^{-i\varphi} & 0 \\ 0 & 1 \end{pmatrix}, \quad (13)$$

to give

$$\mathcal{H}'=\begin{bmatrix} \frac{\hbar^2k^2}{2m}-\hbar\omega_c+\frac{\hbar\omega_s}{2}+\frac{\gamma\hbar^2}{2m^*k_F}\left(\frac{2}{3}\right)^{1/2}k_2\frac{3k_1^2-k_2^2}{2} & \frac{-\gamma}{2}\frac{\hbar^2}{m^*k_F}\frac{k^3}{2\sqrt{3}} \\ \frac{-\gamma}{2}\frac{\hbar^2}{m^*k_F}\frac{k^3}{2\sqrt{3}} & \frac{\hbar^2k^2}{2m}-\frac{\hbar\omega_s}{2}-\frac{\gamma\hbar^2}{2m^*k_F}\left(\frac{2}{3}\right)^{1/2}k_2\frac{3k_1-k_2}{2} \end{bmatrix}$$

$$=\hbar\omega_c\begin{pmatrix} n-\mu+(\frac{2}{3})^{1/2}(\frac{1}{4}\gamma)i(a^3n^{-1/2}-n^{-1/2}a^{+3}) & \gamma n/2\sqrt{3} \\ \gamma n/2\sqrt{3} & n+\mu-(\frac{2}{3})^{1/2}(\frac{1}{4}\gamma)i(a^3n^{-1/2}-n^{-1/2}a^{+3}) \end{pmatrix}. \quad (14)$$

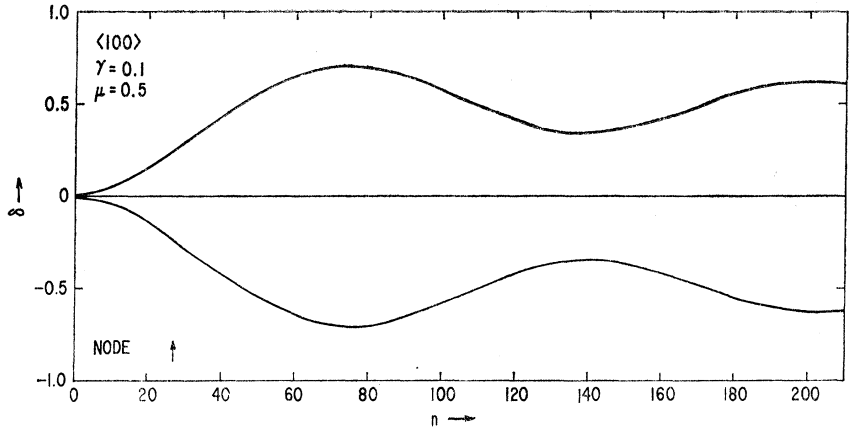

FIG. 2. Deviation of magnetic energy levels for a band with inversion asymmetry splitting from those of a spherical band, plotted in units of $\hbar\omega_c$ against the magnetic quantum number n, for $\mathbf{B}\|\langle 100\rangle$. The two curves represent two sets of levels. The node in the SdH amplitude is shown by the arrow.

Here we have canceled one $k=(2eBn/\hbar c)^{1/2}$ against k_F. Once again we wish to transform one of the orbits to a circle. This time we simply do so to first order in γ, as the large n case has beats already so that we do not need to equate the eigenvalues of the diagonal terms. We have, therefore,

$$\mathcal{H}''=\hbar\omega_c\begin{pmatrix} n-\mu+(\frac{1}{6})\gamma i(a^3n^{-1/2}-n^{-1/2}a^{+3}) & \gamma\hbar/2\sqrt{3} \\ \gamma n/2\sqrt{3} & n+\mu \end{pmatrix}. \tag{15}$$

This Hamiltonian has much the same structure as the $\langle 100\rangle$ case, except that the coupling is between n and $n\pm 3$. The infinite determinant analogous to Eq. (11) has nonvanishing elements in the same places, and the expression for the determinant D_n truncated at n is readily found:

$$D_n'=\{(n+\mu-\lambda)(n-\mu-\lambda)-\tfrac{1}{12}\gamma^2n^2\}D_{n-3}' -\{\tfrac{1}{6}\gamma^2(n-1)(n-2)(n+\mu-\lambda) \times(n-3+\mu-\lambda)\}D_{n-6}'. \tag{16}$$

The roots of Eq. (16), truncated in a manner similar to the $\langle 100\rangle$ case, then give the eigenvalues of Eq. (15) to the desired accuracy.

RESULTS AND DISCUSSION

To give the over-all behavior of the levels, we calculated the eigenvalues for $\gamma=0.1$, $\mu=0.5$ (i.e., no spin splitting), for n up to about 200, at which point the capacity of the computer was reached. The eigenvalues are close to successive integers and we can label them $\epsilon_1(n)$ and $\epsilon_2(n)$. For $\gamma=0$, we would have $\epsilon_1(n)=\epsilon_2(n)=(n+\frac{1}{2})\hbar\omega_c$, the double degeneracy being due to spin splitting. A simple way of representing the levels is to plot versus n the difference between the levels and the $\gamma=0$ values:

$$\epsilon_1(n)=[n+\tfrac{1}{2}+\delta_1(n)]\hbar\omega_c,$$
$$\epsilon_2(n)=[n+\tfrac{1}{2}+\delta_2(n)]\hbar\omega_c. \tag{17}$$

In Fig. 2, we have plotted δ_1 and δ_2 for the $\langle 100\rangle$ case. The nodes in the SdH effect occur for $\delta_1-\delta_2=\frac{1}{2}$, modulo 1, in which case the two sets of levels are interleaved. We see that there is only one actual node, marked by

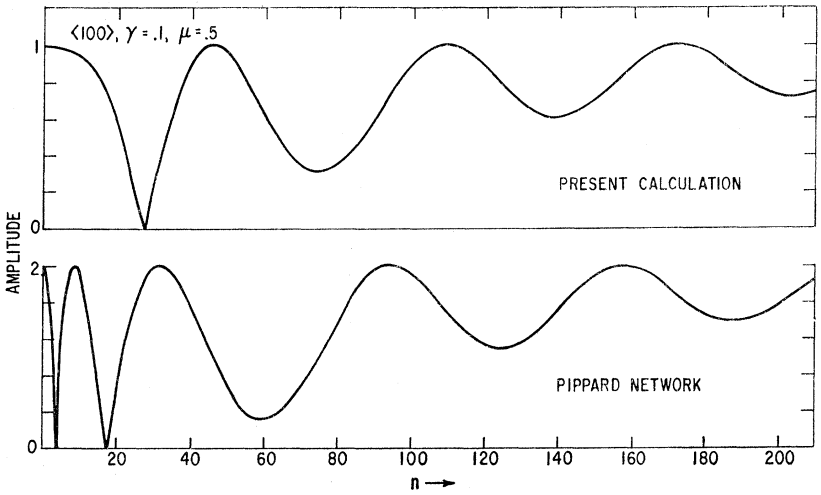

FIG. 3. SdH amplitude versus magnetic quantum number n, compared with Pippard network result. Notice wobble representing partial reverse magnetic breakdown.

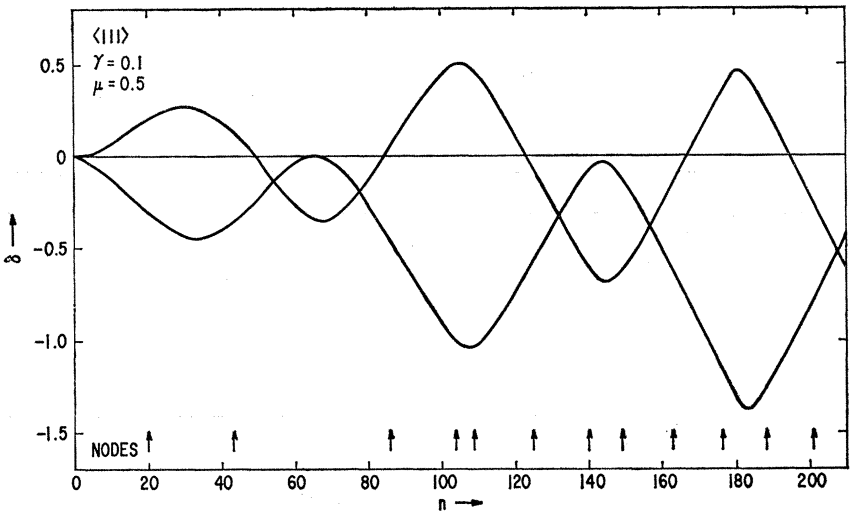

FIG. 4. Deviation of magnetic energy levels for band with inversion asymmetry splitting from those of a spherical band, plotted in units of $\hbar\omega_c$ against the magnetic quantum number n, for $\mathbf{B}\|\langle 111\rangle$. The two curves represent two sets of levels, and nodes in the SdH amplitude are shown by arrows.

an arrow, so that the region of "reverse magnetic breakdown" is rather small. This is what we had suspected in I from an examination of the reverse breakdown parameter. However, for large n, a rather clear cut example of partial breakdown appears, i.e., a wobble in the levels, and so in the de Haas–van Alphen dHvA amplitude, with a long period. Since the total difference in area between the ⟨100⟩ inner and outer orbits in Fig. 1 in I is $2\gamma/\pi$ relative to the original area, the corresponding beat period is $\pi/2\gamma$ oscillations$=15.7$ for $\gamma=0.1$. The period of the wobble in Fig. 2 is 128 oscillations, which is very close to 125.6 or eight times the above total area difference beat period.

It is perhaps more interesting to look at the SdH amplitude itself. The modulation of the fundamental amplitude[7] due to inversion asymmetry splitting is given by the function

$$A_n=\cos\pi(\delta_1-\delta_2). \tag{18}$$

This is plotted in Fig. 3 and we see that the period of the amplitude variation is 64 oscillations or four times the total area difference beat period, which is the same

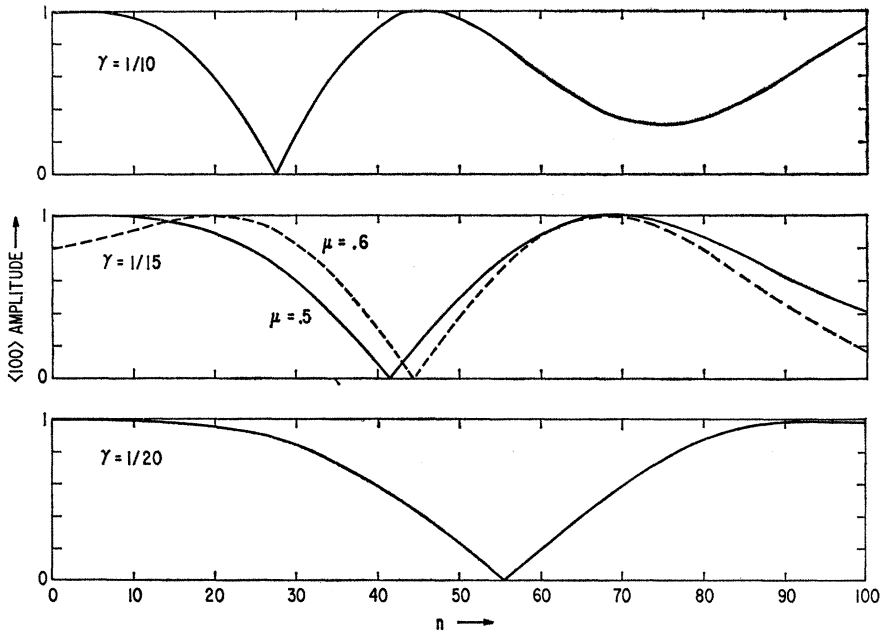

FIG. 5. SdH amplitude versus magnetic quantum number n for $B\|\langle 100\rangle$; where not indicated, $\mu=0.5$.

[7] We are assuming that the dHvA results for the fundamental amplitude apply to the SdH effect. For the general theory of these effects and for further references, see L. M. Roth and P. N. Argyres, in *Semiconductors and Semimetals*, edited by R. K. Willardson and A. C. Beer (Academic Press Inc., New York, 1966), Vol. 1.

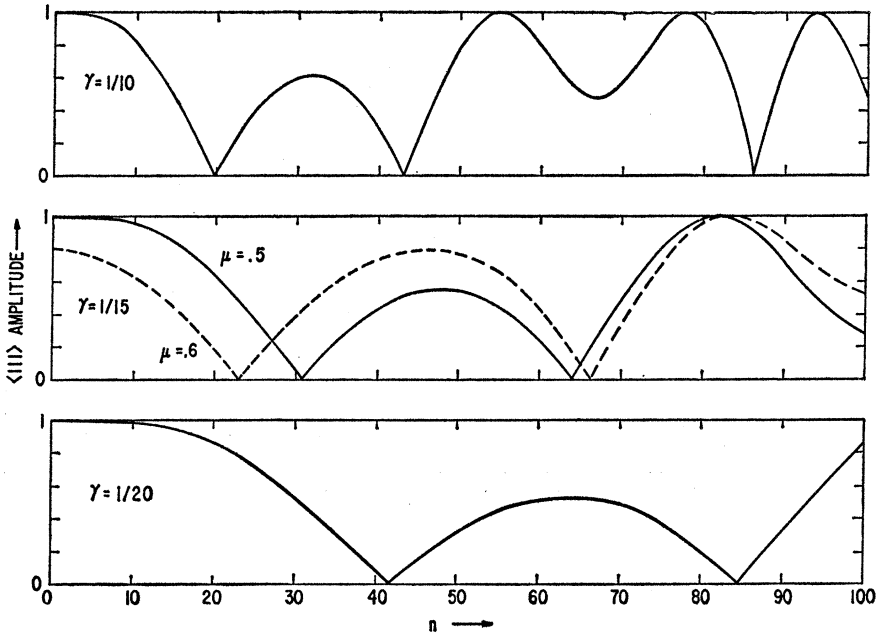

FIG. 6. SdH amplitude versus magnetic quantum number n for $B\|\langle 111\rangle$; where not indicated, $\mu=0.5$.

as the prediction of I. In I we used a Pippard[8] network analysis, and the result for the same parameters is also shown in Fig. 4 for comparison with the present calculation. We see that the results are rather similar for the partial breakdown region, but quite different for very small n where the Pippard network analysis gives an extra node. This verifies our suspicion that for small n the WKB type of analysis breaks down.

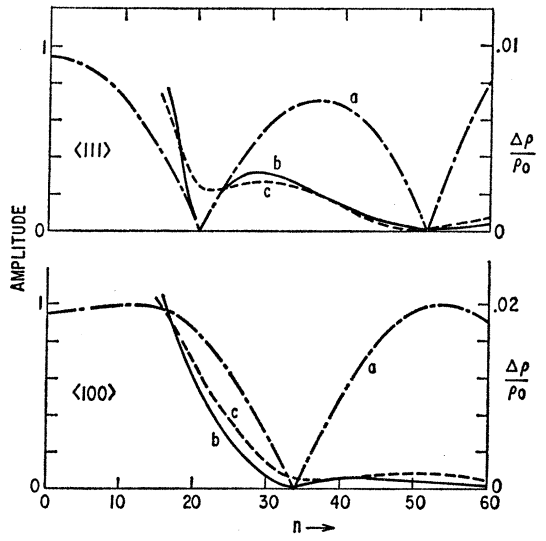

FIG. 7. Comparison of theory and experiment for SdH amplitude: (a) Theory with $\gamma=0.85$, $\mu=0.55$. (b) Theoretical results multiplied by $\exp(-0.0978n)$ to approximate thermal damping. The scale is just the $\Delta\rho/\rho$ scale with the readings multiplied by ten. (c) Whitsett's experimental curves for 1.2° from Fig. 1. The plot against magnetic quantum number is equivalent to plotting against B^{-1} in units of the SdH period.

Turning now to the ⟨111⟩ case, we have plotted δ_1 and δ_2 versus n for $\gamma=0.1$ and $\mu=0.5$ in Fig. 4. There are now many nodes, marked by arrows. We see that for large n, the nodes are becoming equally spaced, and that the straight line portions of the plot, which are classical, are becoming more dominant. Actually the classical picture would consist simply of straight lines, but there is a switching over from one set to another due to the coupling. For the region of experimental interest, we notice a serious departure from the classical result, i.e., a breakdown effect. This is ordinary magnetic breakdown. The separation of the first two nodes is just double the classical value. This finding therefore invalidates the classical picture which we used previously to determine γ, so that our result for that parameter will be different. In I we defined a breakdown parameter s^2 [see the paragraph containing Eq. (11) and also Blount[9]], and we can calculate this parameter for the ⟨111⟩ case, giving $s^2=6^{-3/2}\pi\epsilon_F\gamma/\hbar\omega_c$. For s^2 large we have classical results. For the case of Fig. 2, s^2 becomes 1 at about $n=50$, so that it is not surprising that we are in the breakdown region.

In order to compare our results with experiment we calculated the amplitude function [Eq. (18)] for several values of γ and for $n<100$. This is shown in Figs. 5 and 6. We see that in each case the pattern almost scales with γ, the position of the nodes changing linearly with $1/\gamma$. We have also investigated the effect of including a finite, negative g factor, and the result for

[8] A. B. Pippard, Proc. Roy. Soc. (London) A270, 1 (1962).

[9] E. I. Blount, Phys. Rev. 126, 1636 (1962).

$\mu=0.6$ is shown in the dashed curve. We see that the nodes are shifted slightly by the spin splitting.

In attempting to match the experimental results of Whitsett's sample L as shown in Fig. 1, we found that the parameters $\gamma=0.089$, $\mu=0.53$ gave the correct positions ($n=21$ and 49) of the nodes in the ⟨111⟩ case, while the 100 node turned out to be at $n=32$. This is between the two ⟨111⟩ nodes but is too low by five oscillations. Thus the theory gives the correct result qualitatively but is not in complete quantitative agreement with experiment. A compromise calculation is shown in Fig. 7 for the parameters $\gamma=0.085$ and $\mu=0.55$. We have also plotted the amplitude including an exponential damping factor to aid comparison with the experimental results as shown.

A possible reason for the discrepancy between the ⟨100⟩ and ⟨111⟩ results lies in the neglected anisotropic terms in the Hamiltonian, i.e., the warping terms and g factor. In connection with the g factor, Booth and Ewald[10] have found from the splitting of SdH peaks in grey tin that the g factor for the conduction band of that material varies considerably with magnetic field direction. For a concentration of 2.5×10^{18} cm^{-3}, the magnitude of the g factor changed from 17.0 in the ⟨100⟩ direction to 7.5 in the ⟨111⟩ direction. Since carrying out the present calculation we also became aware of the work of Blick and Landwehr[11] who studied the dHvA effect in HgSe using high magnetic fields for $B\|\langle100\rangle$. They found a g factor of about 12 in magnitude for this concentration sample, which with $m^*=0.049m$ corresponds to $\mu=\frac{1}{2}(1-9m^*/2m)=0.65$, if we assume that g is negative. The above results suggest that we should be using a larger value for μ, and possibly different values of μ for different directions, although this goes beyond the limits of our theory. If we simply increase μ to 0.65 for the ⟨100⟩ case, the node is moved by several oscillations in the right direction. It would be desirable to include anisotropy in the theory, but we have thus far not succeeded in doing so.

As for the magnitude of γ, if we take the compromise value of 0.085, the result implies that the maximum radial splitting of the two energy surfaces is 4.2%. The area difference between the two classical orbits in the ⟨111⟩ direction is found by numerical integration to be 0.80γ, or 6.8%, which is about double that expected from using the classical theory. In I we quoted a result for the maximum energy splitting for the same sample of 5% of the Fermi energy or 7 meV. This was, it turned out, in error by a factor of 2 and should have been $2\frac{1}{2}$%. The calculation quoted showed that in this range of carrier density the percentage energy splitting is about equal to the percentage area splitting, rather than double it, due to nonparabolicity. Our result for the maximum energy splitting is therefore 4 to 5%, which, in fact, about coincides with the result originally quoted.

TABLE I. Positions of nodes in Whitsett's[a] SdH measurements for n-type HgSe.

Electron concentration (cm^{-3})	k_F (10^6 cm^{-1})	n value of nodes ⟨111⟩ Node 1	⟨111⟩ Node 2	⟨100⟩ Node
8.46×10^{17}	2.92	16	[b]	35
1.34×10^{18}	3.40	21	49	38
4.52×10^{18}	5.10	[b]	47	36

[a] See Ref. 2.
[b] Beyond experimental range.

At this point, it is interesting to discuss certain features of the experimental results in the light of the theory. First, the n value of the nodes as a function of concentration is presented in Table I. We see that there is not a drastic dependence upon concentration, the largest change being in the first ⟨111⟩ node. This change is probably partly due to a decrease of μ with increasing concentration which is in turn due to a decrease of the magnitude of the negative g factor. But the indication is that γ is also decreasing with increasing concentration. This may be evidence for a linear dependence on k in the inversion asymmetry splitting. Such a linear dependence is possible if the band structure of HgSe is of the grey tin type,[1,3,4,12] for which there is some evidence.[12] It would be interesting to see a more complete experimental study of the concentration dependence of the nodes.

For lower concentrations, clear-cut nodes were not observed. However, n only goes up to 16–18 for the two lower concentration samples (Figs. 2 and 3 of Whitsett's article[2]), so that for ⟨100⟩ we certainly do not expect a node. For ⟨111⟩ there is a flattening of the curve in the vicinity of 16 which may be the beginning of a node and this merits further investigation. In the ⟨100⟩ sample EE ($N=3.47\times10^{17}$ cm^{-3}) there occurs a minimum in the amplitude at $n=8$. It is possible that this is related to the fact that when a negative g factor is included, the amplitude increases for small n (see Fig. 6), and this coupled with thermal damping may produce a minimum. Unfortunately, this does not explain why the effect does not occur for sample N ($N=2.08\times10^{17}$ cm^{-3}).

In conclusion, the exact calculation of magnetic energy levels in a band with inversion asymmetry splitting shows that this effect can explain the beating observed in the SdH effect in HgSe. Recent measurements of the oscillatory magnetoresistance in GaSb by Seiler and Becker[13] show a similar beating pattern, which is also believed to be due to inversion asymmetry. We hope to present an analysis of these results in the near future. It will be interesting to see whether the effect is observed in other materials.

[10] B. L. Booth and A. W. Ewald Phys. Rev. **168**, 805 (1968).
[11] L. M. Blick and G. Landwehr, in *II-VI Semiconducting Compounds, 1967 International Conference*, edited by D. A. Thomas (W. A. Benjamin, Inc., New York, 1967), p. 879.
[12] S. H. Groves, R. N. Brown, and C. R. Pidgeon, Phys. Rev. **161**, 779 (1967).
[13] D. G. Seiler and W. M. Becker, Phys. Letters **26A**, 96 (1967).

ACKNOWLEDGMENT

This work is a continuation of a study by S. Groves and P. Wyatt to explain the HgSe beat frequency. Whitsett suggested that the beat frequency pattern could be explained qualitatively by adding bulges along the ⟨111⟩ directions to the spherical Fermi surface. Groves and Wyatt showed that the warping for either a Γ_8 or a Γ_6 conduction band did produce the distortion of the Fermi sphere desired by Whitsett; however, they found that the large amount of warping needed to produce the double frequencies was incompatible with the near isotropy of the high-frequency oscillations. They then turned to the inversion asymmetry splitting as a possible explanation, and showed that if the ⟨111⟩ beat frequency was used to find the difference area for these directions the resulting zinc-blende splitting was not unreasonable in size. However, the uncertainty of the proper orbits and frequencies for the ⟨100⟩ and ⟨110⟩ directions held this explanation of the beating in doubt, and motivated the theoretical work on the orbits and magnetic energy levels by the author reported in I and this paper. It is a pleasure to thank S. Groves for calling attention to this problem and for subsequent discussions.

PHYSICAL REVIEW VOLUME 173, NUMBER 3 15 SEPTEMBER 1968

Optical Absorption due to Inter-Conduction-Minimum Transitions in Gallium Arsenide

IVAR BALSLEV*
Bell Telephone Laboratories, Murray Hill, New Jersey
(Received 16 April 1968)

The infrared absorption in *n*-type GaAs has been studied as function of carrier concentration, temperature, and uniaxial stress. The data have established that the lowest secondary minima are located at the Brillouin-zone edge along $\mathbf{k}\|\langle 001\rangle$, 0.43±0.015 eV above the $\mathbf{k}=0$ minimum at 80°K. An observed structure near 0.7 eV has been assigned to transitions into a higher-lying ⟨100⟩ minima 0.78±0.05 eV above the primary minimum. The spectra revealed no evidence of transitions to ⟨111⟩ minima.

INTRODUCTION

THE exploration of secondary conduction-band minima has attracted considerable interest for two reasons. First, such minima can be important for high-field transport properties, and second, an experimental determination of their position in energy and $\mathbf{k}$ space is valuable in the comparison with band calculations. The conduction band in GaAs is characterized by a lowest minimum at $\mathbf{k}=0$ and by sets of equivalent minima at X and L of the zone boundary. Different types of band calculations[1–3] indicate that these secondary minima occur 0.2–0.6 eV above the primary minimum. A separation of 0.36 to 0.38 eV between primary and lowest secondary minimum has been derived from transport measurements,[4–6] whereas infrared measurements by Spitzer and Whelan[7] (SW) were interpreted by Haga and Kimura[8] (HK) to give a separation of 0.44 eV. The influence of uniaxial stress on Gunn effect[9] and some properties of GaAs GaP alloys, e.g., Gunn effect[9] and optical absorption edge,[10] have established that the lowest secondary minimum is located at X, the optical studies indicating a separation of 0.4 eV.[10] It is further known that a set of valleys with symmetry X_3 have extremum energies 0.33 eV above the lower X_1 minima.[1] So far, there has been no experimental determination of the position of the L valleys, but dependence of the Gunn threshold on high [111] uniaxial stress[9] seems to indicate that these valleys are located at least 0.1 eV above the Gunn active valleys.[11]

In this paper we shall report on measurements similar to those of SW,[7] i.e., studies of near-infrared

* Present address: Physics Laboratory III, Technical University of Denmark, Lyngby, Denmark.

[1] M. Cardona, K. L. Shaklee, and F. H. Pollak, Phys. Rev. **154**, 696 (1967).

[2] M. L. Cohen and T. K. Bergstresser, Phys. Rev. **141**, 789 (1966).

[3] F. Herman, R. L. Kortum, C. D. Kuglin, and J. L. Shay, in *II–VI Semiconducting Compounds*, edited by D. G. Thomas (W. A. Benjamin, Inc., New York, 1967), p. 503.

[4] J. M. Whelan and G. H. Wheatley, J. Phys. Chem. Solids **6**, 169 (1958); L. W. Aukerman and R. K. Willardson, J. Appl. Phys. **31**, 293 (1960).

[5] H. Ehrenreich, Phys. Rev. **120**, 1951 (1960).

[6] A. R. Hutson, A. Jayaraman, and A. S. Coriell, Phys. Rev. **155**, 786 (1967).

[7] W. G. Spitzer and J. M. Whelan, Phys. Rev. **114**, 59 (1959).

[8] E. Haga and H. Kimura, J. Phys. Soc. Japan **19**, 1596 (1964).

[9] M. Shyam, J. W. Allen, and G. L. Pearson, IEEE Trans. Electron Devices **13**, 63 (1966).

[10] D. Madelung, *Physics of III–V Compounds* (John Wiley & Sons, Inc., New York, 1964), p. 351.

[11] A. R. Hutson has pointed out that the small dimensions parallel to the stress used in Ref. 9 lead to uniaxial strain rather than uniaxial stress. When inserting appropriate elastic constants it is estimated that a [111] stress yields a volume change of 0.60 rather than $\frac{1}{3}$ times that of a similar hydrostatic pressure. This removes the discrepancy mentioned in Ref. 9, and there is no evidence of a crossing for high [111] stresses between the X valleys and the lowest L valley.